Experiments with acoustic solitons in crystalline solids

H.-Y. Hao and H. J. Maris
Department of Physics, Brown University, Providence, Rhode Island 02912
(Received 26 February 2001; published 18 July 2001)

We have used the picosecond ultrasonic technique to study the formation of acoustic solitons. In these experiments, a longitudinal acoustic pulse is generated at one surface of a sample. After the pulse has propagated across the sample, its shape is modified as a result of phonon dispersion and nonlinearity. We have found that the change in the pulse shape can be described by the Korteweg–de Vries equation. The experiments have been performed on Si, MgO, α-quartz, and sapphire. For each sample, we have observed fully developed acoustic solitons, with pulse shapes that are in reasonable agreement with the results of computer simulations.

DOI: 10.1103/PhysRevB.64.064302 PACS number(s): 63.20.−e

I. INTRODUCTION

In a nonlinear dispersive system, an initial disturbance can evolve into a solitary wave that retains its shape over a long distance. In 1834, John Scott Russell observed a solitary wave on the water surface in a narrow channel.[1] Korteweg and De Vries (KdV) provided a theoretical analysis of this wave in 1895.[2] But it was not until 1965, when the particle-like behavior of the solitary-wave solutions in the KdV equation was found, that Zabusky and Kruskal[3] termed these solutions solitons. It has been found that when solitons collide with each other, they resume their initial wave forms and speeds. Since this discovery, there have been many theoretical and experimental studies of the behavior of solitons in a wide range of nonlinear systems. By developing and applying the inverse scattering transform,[4] mathematicians have found soliton solutions in other nonlinear evolution equations, including the nonlinear Schrödinger equation and the sine-Gordon equation. Experimentalists have also observed the formation and interactions of solitons in a wide range of systems, including shallow water, transmission lines, plasmas, and optical fibers.

In this paper we study acoustic solitons in crystalline solids. In this system the dispersion arises from the finite spacing of the atoms, and the non-linearity comes from the anharmonicity of the interatomic forces. We first introduce the nonlinear wave equation that governs the propagation of finite-amplitude acoustic waves in crystals and discuss the conditions for solitons to form. We then describe ultrasonic experiments that we have performed to test the theory. Measurements have been performed on Si, MgO, quartz, and sapphire.

II. THEORY OF ACOUSTIC SOLITONS: WAVE EQUATION

In this section, we derive the wave equation that governs the propagation of a finite amplitude acoustic wave in a dispersive crystalline solid. For a wave of wavelength sufficiently long that the effect of dispersion can be ignored, we can use standard nonlinear elasticity theory[5,6] to derive the following wave equation:

$$\rho_0 \frac{\partial^2 u_\alpha}{\partial t^2} = \frac{\partial^2 u_\gamma}{\partial a_\beta \partial a_\delta}\left(A_{\alpha\beta\gamma\delta} + A_{\alpha\beta\gamma\delta\epsilon\zeta}\frac{\partial u_\epsilon}{\partial a_\zeta}\right), \tag{1}$$

where a_α is the material coordinate in the α direction (Lagrangian coordinate), u_α is the displacement in this direction, ρ_0 is the density in the undeformed state, and the coefficients $A_{\alpha\beta\gamma\delta}$ and $A_{\alpha\beta\gamma\delta\epsilon\zeta}$ are defined by

$$A_{\alpha\beta\gamma\delta} = C_{\alpha\beta\gamma\delta}, \tag{2}$$

$$A_{\alpha\beta\gamma\delta\epsilon\zeta} = C_{\alpha\beta\gamma\delta\epsilon\zeta} + C_{\alpha\beta\delta\zeta}\delta_{\gamma\epsilon} + C_{\gamma\delta\beta\zeta}\delta_{\alpha\epsilon} + C_{\epsilon\zeta\beta\delta}\delta_{\alpha\gamma}, \tag{3}$$

with $C_{\alpha\beta\gamma\delta}$ and $C_{\alpha\beta\gamma\delta\epsilon\zeta}$ second and third order elastic constants, respectively.[7] This equation includes nonlinear effects to just the lowest order; terms that are of third or higher order in the displacement are neglected.

In this paper we restrict attention to the propagation of longitudinal waves in a direction of high symmetry, such as one of the principal directions in a cubic crystal. The displacement of the wave will then be in the direction of propagation, and Eq. (1) reduces to a scalar equation

$$\rho_0 \frac{\partial^2 u}{\partial t^2} = \left(C_2 + C_3 \frac{\partial u}{\partial a}\right)\frac{\partial^2 u}{\partial a^2}, \tag{4}$$

where u and a are the displacement and the material coordinate, respectively, in the direction in which the wave is propagating, and C_2 and C_3 are combinations of second and third order elastic constants. Examples of these combinations are listed in Table I.

To include the effect of dispersion, we first note that for long wavelengths the phonon dispersion relation can be expanded in the form

$$\omega = ck - \gamma k^3 + \cdots \tag{5}$$

or

$$\omega^2 = c^2k^2 - 2c\gamma k^4 + \cdots, \tag{6}$$

where $c = (C_2/\rho_0)^{1/2}$ is the sound velocity, k is the wave number, and γ is a constant that is usually positive. We would like to modify the wave equation [Eq. (4)] so that for waves of small amplitude the dispersion relation is as given

TABLE I. Values of the coefficients C_2 and C_3 appearing in Eq. 8 for different propagation directions.

Direction	C_2	C_3
cubic [100]	C_{11}	$C_{111}+3C_{11}$
cubic [110]	$\frac{1}{2}(C_{11}+C_{12}+2C_{44})$	$\frac{1}{4}(C_{111}+3C_{112}+12C_{166})+\frac{3}{2}(C_{11}+C_{12}+2C_{44})$
cubic [111]	$\frac{1}{3}(C_{11}+2C_{12}+4C44)$	$\frac{1}{9}(C_{111}+6C_{112}+12C_{144}+24C_{166}+2C_{123}+16C_{456})$ $+(C_{11}+2C_{12}+4C_{44})$
trigonal [0001]	C_{33}	$C_{333}+3C_{33}$

by Eq. (5). This can be achieved through inclusion of a fourth order spatial derivative, so that the wave equation then becomes

$$\rho_0 \frac{\partial^2 u}{\partial t^2} = \left(C_2 + C_3 \frac{\partial u}{\partial a} \right) \frac{\partial^2 u}{\partial a^2} + 2\rho_0 c \gamma \frac{\partial^4 u}{\partial a^4}. \tag{7}$$

It is useful to consider the relation of this equation to an equation that has the KdV form. Let us define the strain $\eta \equiv \partial u/\partial a$. By differentiation of Eq. (7) with respect to a, we obtain

$$\rho_0 \frac{\partial^2 \eta}{\partial t^2} = C_2 \frac{\partial^2 \eta}{\partial a^2} + C_3 \frac{\partial}{\partial a}\left(\eta \frac{\partial \eta}{\partial a} \right) + 2\rho_0 c \gamma \frac{\partial^4 \eta}{\partial a^4}. \tag{8}$$

Now we consider an equation of the KdV form

$$\frac{\partial \eta}{\partial t} = -B_1 \frac{\partial \eta}{\partial a} - B_2 \eta \frac{\partial \eta}{\partial a} - B_3 \frac{\partial^3 \eta}{\partial a^3}, \tag{9}$$

where B_1, B_2, and B_3 are some coefficients to be determined. We differentiate Eq. (9) with respect to time, and use Eq. (9) again to replace the time-derivatives of the strain that appear on the right-hand side. The result is

$$\frac{\partial^2 \eta}{\partial t^2} = B_1^2 \frac{\partial^2 \eta}{\partial a^2} + 2B_1 B_2 \frac{\partial}{\partial a}\left(\eta \frac{\partial \eta}{\partial a} \right) + 2B_1 B_3 \frac{\partial^4 \eta}{\partial a^4} + \cdots. \tag{10}$$

The higher order terms omitted from the right hand side of this equation involve the sixth order derivative of η, terms of the order of η^3 , or products of the form $(\partial^i \eta/\partial a^i) \times (\partial^j \eta/\partial a^j)$, where $i+j \geqslant 4$. Thus, these are all higher order than the terms that are retained. If the B_n coefficients are chosen to have the values

$$B_1 = (C_2/\rho_0)^{1/2} = c, \quad B_2 = C_3/2\rho_0 c, \quad B_3 = \gamma, \tag{11}$$

then Eq. (10) becomes identical to Eq. (8). It follows that if this choice of the coefficients is made, the solutions of Eq. (9) will also be solutions of Eq. (8), although not all solutions of Eq. (8) will be solutions of Eq. (9). The solutions of Eq. (9) correspond to disturbances that propagate in the positive direction along the a axis. It is also possible to choose instead $B_1 = -c$, together with appropriate choices of B_2 and B_3. Then the solutions of Eq. (9) are disturbances that propagate in the negative direction.

It follows that we can find solutions of the generalized elastic wave equation [Eq. (7)] by taking over known solutions of the KdV equation. The KdV equation has two classes of special solution. The first are periodic solutions, *cnoidal* waves, and the second class are the solitons. Since in our experiments, we will be considering an initial disturbance that is a short acoustic pulse, we will focus on the properties of the soliton solutions. It is well known that Eq. (9) has a soliton solution[8–10]

$$\eta = \eta_0 \operatorname{sech}^2\left\{ \left(\frac{B_2 \eta_0}{12 B_3} \right)^{1/2} (a - Ut) \right\}$$

$$= \eta_0 \operatorname{sech}^2\left\{ \left(\frac{C_3 \eta_0}{24 \rho_0 c \gamma} \right)^{1/2} (a - Ut) \right\}, \tag{12}$$

$$U = c + \frac{B_2 \eta_0}{3} = c + \frac{C_3 \eta_0}{6\rho_0 c}, \tag{13}$$

where U is the velocity of the soliton and η_0 is the peak strain amplitude. Since B_2 is normally negative and B_3 is positive, we see from Eq. (12) that η_0 must be negative, i.e., the pulse must be a compression, rather than a rarefaction. The soliton velocity U is always larger than the sound speed c. Note that the magnitude of the dispersion does not affect the velocity, but only influences the width of the soliton.

The KdV solitons are stable, and an initial pulse of arbitrary shape can evolve into one or more solitons. The number of solitons formed from a particular initial pulse shape can be found from the inverse scattering transform.[8–10] The number of solitons is the same as the number of bound states of the associated Schrödinger equation

$$\frac{d^2 \Psi}{da^2} + [E - V(a)]\Psi = 0, \tag{14}$$

where the potential $V(a)$ is related to the initial pulse shape $\eta_i(a)$ in the form

$$V(a) = -\frac{B_2 \eta_i(a)}{6B_3} = -\frac{C_3 \eta_i(a)}{12\rho_0 c \gamma}. \tag{15}$$

As a specific example, consider an initial disturbance in which the strain has the value $-\eta_1$ between $a=0$ and $a=w$ and is zero elsewhere.[11] From the Schrödinger equation, we know that provided η_1 is positive, there will always be at least one bound state, and that there will be n bound states if

$$(n-1)^2 \leqslant \frac{C_3 w^2 \eta_1}{12\pi^2 \rho_0 c \gamma} \leqslant n^2. \tag{16}$$

TABLE II. A list of samples that were used in the experiments, together with their material parameters. The dispersion parameter γ and the nonlinear parameter C_3 are as defined in Eqs. (5) and (4), respectively. The density, sound velocity, and nonlinear parameter are calculated from the data in Refs. 15–17. The dispersion parameters are from Ref. 18.

Sample	Sample thickness d (cm)	Density ρ_0 (g cm^{-3})	Sound velocity c (10^5 cm s^{-1})	Nonlinear parameter C_3 (10^{12} g cm^{-1} s^{-2})	Dispersion parameter γ (10^{-11} cm^3 s^{-1})
Si [100]	0.0315	2.33	8.48	-3.73	1.80
MgO [100]	0.0495	3.585	9.05	-40.2	1.6
SiO_2 [0001]	0.2010	2.651	6.40	-4.88	7.75
Al_2O_3 [0001]	0.1065	3.98	11.23	-18.3	3.50

From this result, we can make a rough estimate of the experimental conditions necessary in order for multiple solitons to appear. Of particular interest is the magnitude and spatial length of the strain pulse that is required. The material parameters of the samples that we have studied are listed in Table II. As a representative case, consider the propagation in the [100] direction of silicon of a strain pulse that initially has a width of 200 Å. From Eq. (16), we find that in order for two solitons to be produced, the magnitude η_1 of the strain must exceed 2.8×10^{-4}. The critical strain varies significantly between the different materials; the smallest critical strain is 3.8×10^{-5} for MgO.

To design an experiment, it is also necessary to consider the distance a pulse has to propagate before a soliton can be observed. Consider, again an experiment in which the starting situation is a strain $-\eta_1$ extending over distance w. Suppose that one soliton is produced. For simplicity, we assume that the disturbance develops in a way such that the soliton becomes the dominant contribution to the strain distribution, i.e., we suppose that the amplitudes of the disturbances occurring behind the soliton are small. When the strain pulse is launched the relative displacement of the material in front and behind the pulse is $w\eta_1$. If the attenuation is negligible, this relative displacement will be conserved, and so must be equal to the relative displacement of the material on either side of the soliton. Using this result, it follows from Eq. (12) that

$$\eta_0=\frac{\eta_1^2 w^2 C_3}{96\rho_0 c\gamma}. \tag{17}$$

The difference between the velocity of the soliton and the velocity of small-amplitude disturbances is given by Eq. (13). Using this velocity difference, we can calculate the propagation distance required in order for the soliton to have traveled an extra distance that is equal to the soliton width $(24\rho_0 c\gamma/C_3\eta_0)^{1/2}$. This propagation distance is

$$d=\frac{27{,}648\rho_0^3 c^4\gamma}{C_3^3\eta_1^3 w^3}. \tag{18}$$

Thus, for Si with $w=200$ Å and a propagation distance d of 500 μm, it is necessary for the initial strain amplitude to have a magnitude of at least

$$\left|27648^{1/3}\frac{\rho_0 c^{4/3}\gamma^{2/3}}{C_3 w d^{1/3}}\right|=6.56\times10^{-4}. \tag{19}$$

This is within the range of strain amplitudes that can be generated in a picosecond ultrasonics experiment.

It is important to recognize that because of the way in which the effect of phonon dispersion has been included, the wave equations (7) and (10) have to be used with care. For example, if the nonlinear coefficient C_3 in Eq. (7) is set equal to zero, this equation becomes a linear wave equation with the dispersion relation $\omega^2=c^2k^2-2c\gamma k^4$. Thus, for large enough k, the waves have a purely imaginary frequency, and the amplitude of the Fourier components with wave number k will grow with time as $\exp[(2c\gamma)^{1/2}k^2t]$. It follows from Parseval's theorem that if the Fourier components of the initial disturbance fall off for large k as a power law, the solution will diverge for any finite value of the time t, i.e., the displacement $u(a)$ and the strain $\eta(a)$ will cease to be a square-integrable function of a. The wave number k_c at which the frequency becomes imaginary is $(c/2\gamma)^{1/2}$, which is of same order of magnitude as the inverse of the lattice parameter. The strain pulses that we use in this experiment have spatial lengths of several hundred Å, and consequently have very small Fourier components with k in the range above k_c. Nevertheless, the solution of Eq. (7) still diverges for all $t>0$. This difficulty can, in principle, be removed by adding into Eqs. (7) and (10) extra terms involving higher order derivatives, and then choosing the coefficients of these terms so that the frequency is real for all values of k. In the present work (see next sections), we solve Eqs. (7) and (10) using numerical simulation with a mesh of points for a. A finite mesh spacing is equivalent to an upper cutoff for k, and so the difficulties with the divergences at large k do not occur.

III. EXPERIMENT

The basic idea of our experiment is to generate a short acoustic pulse, launch it into the sample, and to measure the shape of the pulse after it has made one round trip through the sample. The samples were single crystal wafers of [100] Si, [100] MgO, z-cut sapphire, and quartz, with surfaces highly polished to assure a good acoustic reflection. Parameters of the samples are listed in Table II.

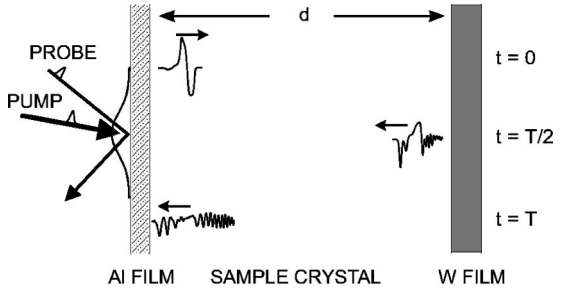

FIG. 1. Schematic diagram of the experiment. A light pulse is absorbed in the Al film and an acoustic pulse is generated. The pulse propagates across the crystal and is reflected at the *W* film. The pulse returns to the Al transducer with a shape modified by dispersion and nonlinearity, and is detected by a probe light pulse.

The experiment is shown schematically in Fig. 1. An Al film was deposited onto one side of the wafer to serve as a transducer for generating and detecting the acoustic pulses. The thickness d_{Al} of the Al film was in the range between 235 to 250 Å. To generate an acoustic pulse, a light pulse (pump pulse) of duration 200 fs from a Ti:sapphire mode-locked laser was focused onto a spot of diameter $\sim 25\ \mu$m on the surface of the Al film. The laser light absorbed in the film raises the film temperature. This sets up a thermal stress in the Al film, and a longitudinal acoustic pulse is launched into the sample. The wavelength of the light pulse was 800 nm, and the time between pulses of 13.25 ns. The returning acoustic pulse results in a change in the optical reflectivity of the Al film; this change in reflectivity was detected by means of a time-delayed light pulse from the same laser (probe pulse). The fractional change of reflectivity $\Delta R(t)/R$ was of the order of 10^{-5}, and so lock-in techniques were used to improve the signal to noise. The travel time for the first acoustic pulse ranged from 70 ns for the Si sample to over 600 ns for SiO_2. It is inconvenient to produce a probe pulse with such a large time delay through the use of a conventional optical path. Instead, as a probe pulse, we used a later pulse from the laser which was given a further delay by means of a short adjustable optical path.

When a strain pulse is generated in the Al film and propagates into the crystal, it will produce a soliton if the amplitude is sufficiently large. As noted in the previous section, the soliton must have a negative strain, i.e., it must correspond to a compression. If this strain pulse were to be reflected at a free surface of the sample, it would undergo a sign change and convert into a rarefaction pulse. The soliton would then be destroyed. To avoid this problem, a 3000 Å film of *W* was deposited onto the far side of the wafer. When the strain pulse is reflected at the interface between the wafer and the *W* film, the reflection coefficient is

$$r=\frac{Z_W-Z_S}{Z_W+Z_S}, \tag{20}$$

where Z_W and Z_S are the acoustic impedances of *W* and the sample, respectively. The very large value of the acoustic impedance of the W results in a large magnitude for the reflection coefficient, and also no change in sign of the strain.

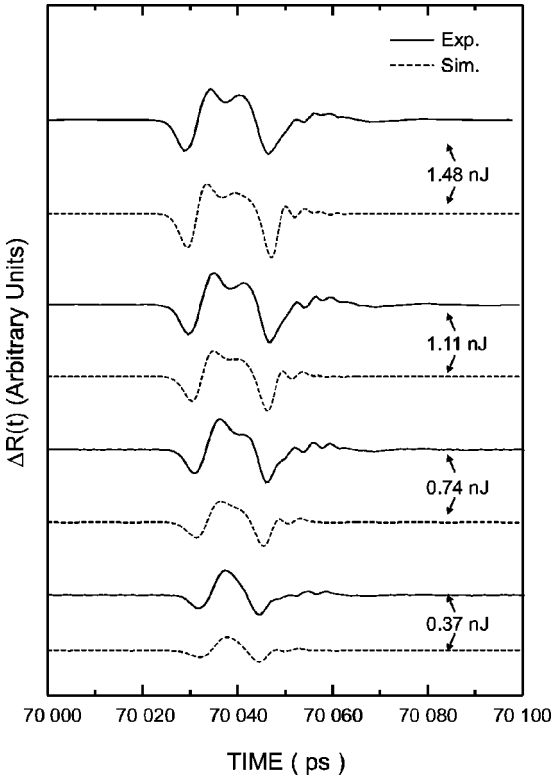

FIG. 2. First strain echo in a [100] Si sample. Results are labeled by the energy of the pump light pulse. The solid line shows the experimental data, and the dashed line indicates the results from a computer simulation. The experiment was performed at 35 K.

At room temperature, the attenuation of sound in the frequency range of interest here (50 to 200 GHz) is very large, and the strain pulse cannot propagate far enough for solitons to form. The attenuation is mainly due to anharmonic interactions with thermal phonons, and becomes small at low temperature. Consequently, we performed the experiments at temperatures 25 to 35 K using a continuous-flow cryostat. Because the sample was mounted in the cryostat, it was not possible to make an accurate determination of the size of the pump and probe beams on the sample surface.

IV. RESULTS AND DISCUSSION

To test the theory discussed in Sec. II, we have made a series of measurements with different pump pulse energies. In Figs. 2–5, we show the results of measurements of $\Delta R(t)$ for the first echo in the different samples, along with computer simulations to be described below. In each figure, data with four different pump pulse energies are presented. Note that the vertical scale is in arbitrary units, but for a given sample the same scale is used for each of the pump pulse energies. Figure 2 shows the data for Si at the temperature of 35 K. When the pump pulse energy Q is below 0.37 nJ, changing the value of Q changes only the amplitude of the echo, but not the shape. For higher pulse energies, the front

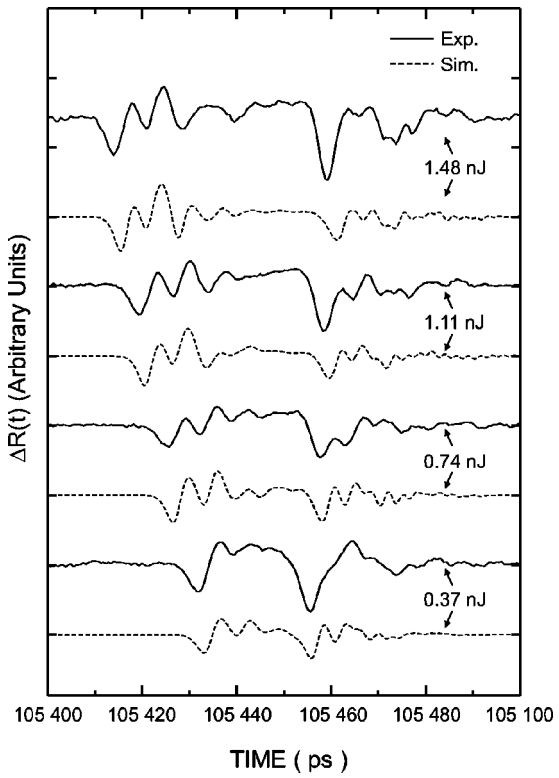

FIG. 3. First echo in a [100] MgO sample. Results are labeled by the energy of the pump light pulse. The solid line shows the experimental data, and the dashed line indicates the results from a computer simulation. The experiment was performed at 30 K.

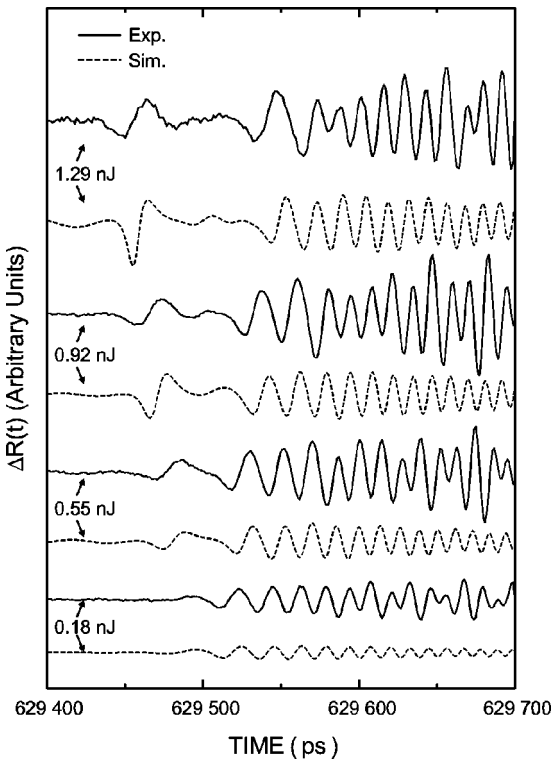

FIG. 4. First echo in a [0001] SiO_2 sample. Results are labeled by the energy of the pump light pulse. The solid line shows the experimental data, and the dashed line indicates the results from a computer simulation. The experiment was performed at 32 K.

of the echo starts to deform. This deformation becomes more significant as Q increases, and eventually a soliton separates from the remainder of the pulse. For the other samples, the threshold pump energy for the formation of a soliton is lower. In MgO, multiple solitons appear at the highest energy, and even for a pulse energy of 0.37 nJ a soliton has clearly separated from the main pulse. For all of the samples, the velocity of the solitons increase with increasing pump power, as expected from Eq. (13). The large number of solitons seen in MgO is expected because of the very large value of the nonlinear parameter C_3 (see Table II).

To calculate the expected shape of the echo requires a determination of the shape of the strain pulse that is generated by the action of the pump light pulse, the modification of the shape of the strain pulse that occurs as it propagates through the sample, and a calculation of the change in optical reflectivity $\Delta R(t)$ that takes place when the strain pulse reenters the Al film.

Let Q be the energy in each pump light pulse, R the optical reflectivity of the Al film, and A the area of the film that is illuminated. Then the energy absorbed per unit area[12] is $Q(1-R)/A$. R was measured to be 0.77. The energy in the pump pulse is transferred to the free electrons in the Al film which diffuse very rapidly through the film before losing their energy to the lattice.[13] As a consequence, it is a good approximation to consider that the temperature rise ΔT of the Al film is uniform throughout its thickness. The thermal stress in the Al film is[14] $\sigma=-3B\beta\Delta T$ where B is the bulk modulus, and β is the linear expansion coefficient. Thus

$$\sigma=-3(1-R)\frac{B\beta Q}{AC}, \tag{21}$$

where C is the specific heat per unit volume. Equation (21) is strictly correct if ΔT is small compared to the ambient temperature; however, if the ratio of β to C is constant, Eq. (21) holds even when ΔT is comparable to the ambient temperature. For Al, the ratio of β to C changes by only 10% over the temperature range 25 to 50 K.

Given the initial value of the thermal stress, it is then straightforward to calculate the form of the strain pulse that is launched into the sample. The detailed shape of this pulse depends on the acoustic reflection coefficient at the interface between the Al film and the sample. This coefficient is determined by the ratio of the acoustic impedance of the Al to the impedance of the sample [see Eq. (20)]. As an example, we show in Fig. 6 the initial shape of the strain pulse generated in MgO. The thickness of the Al film is 250 Å. A film of this thickness generates a strain pulse with Fourier components peaked around 120 GHz.

To calculate the form of the pulse after it has propagated within the sample, we have time developed the strain using the KdV equation [Eq. (9)]. The values of the sound velocity, density, nonlinear elastic coefficient, and dispersion are listed in Table II, and were taken from Refs. 15–18. In Fig. 6 we show, for two different amplitudes of the initial pulse, the form of the strain pulse when it reaches the far side of the

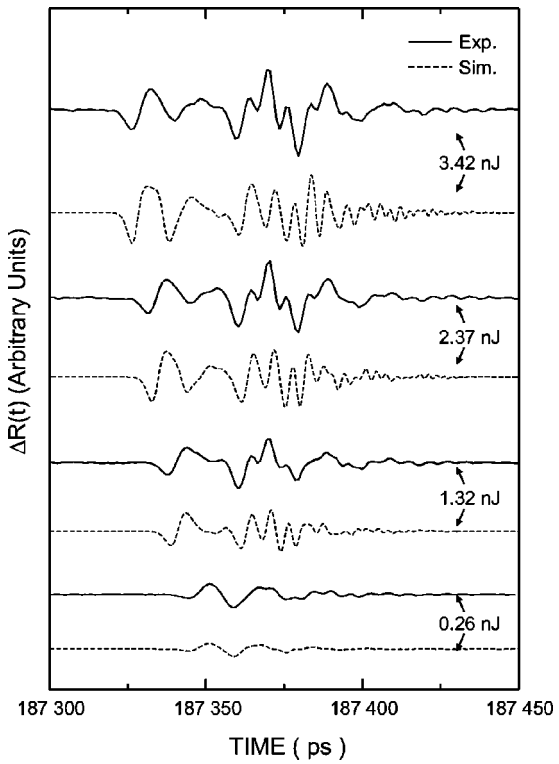

FIG. 5. First echo in a [0001] Al_2O_3 sample. Results are labeled by the energy of the pump light pulse. The solid line shows the experimental data, and the dashed line indicates the results from a computer simulation. The experiment was performed at 35 K.

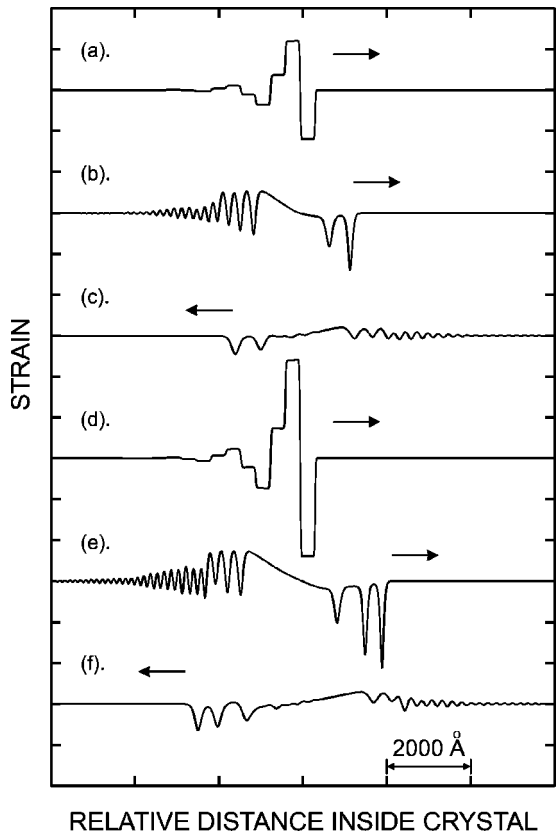

FIG. 6. Computer simulation of the shape of strain pulses propagating in MgO. The upper part of the figure shows (a) the initial pulse entering the sample, (b) the pulse as it approaches the far side of the sample, and (c) as it returns to the Al film. The scale for the strain and distance is as indicated. In the lower part, (d), (e), and (f) show the propagation of a pulse of larger amplitude. The distance scale is as indicated, and each division on the strain axis corresponds to a strain of 5×10^{-5}.

MgO sample. The pulse is then reflected at the interface between the sample and the *W* film. This reduces the amplitude by a factor which for MgO is 0.50. We then continue the time development using the KdV equation, and the results obtained for the pulse when it returns to the Al film are included in Fig. 6. In the simulation of the pulse propagation, the effects of attenuation were included. It was assumed that the attenuation of the different Fourier components in the pulse varied as αk^2, with α a coefficient that varied from sample to sample. Inclusion of the attenuation improves the agreement between the simulation and the data, primarily in the part of the pulse that arrived after the soliton components. It is possible that in the experiment the attenuation does not occur in the bulk of the sample, but instead arises from the roughness of the sample surface.

When the pulse reaches the Al film, a part of it will be reflected back into the sample and a part will enter the film. The part that enters the film will then propagate back and forth across the film. Each time it returns to the interface between the film and the sample, a part of the pulse will be retransmitted into the sample. The time varying strain in the Al film results in a change in the optical constants. From this change, the change in the optical reflectivity of the film can be calculated. To perform this calculation, we used standard values for the optical constants of Al.[19] We write the strain derivative $d\epsilon/d\eta$ of the dielectric constant of Al as $|d\epsilon/d\eta|\exp(i\phi)$. The magnitude of the reflectivity change $\Delta R(t)$ is proportional to $|d\epsilon/d\eta|$, but the shape of $\Delta R(t)$ as a function of time depends only on the phase ϕ.

Of the parameters that enter into the simulation, *A*, $|d\epsilon/d\eta|$, ϕ, and α are not accurately known. The parameter $|d\epsilon/d\eta|$ affects only the magnitude of $\Delta R(t)$. Since, we do not make an absolute measurement of $\Delta R(t)$, the value of $|d\epsilon/d\eta|$ is unimportant. The area *A* over which the pump beam strikes the surface of the sample inside the cryostat is not accurately known. The initial amplitude of the strain pulse is inversely proportional to *A*. When the energy of the pump light pulse is small and nonlinear effects are unimportant, the value of *A* does not have a significant effect on the shape of the returning echo. However, for large pump energy the echo shape is affected by the initial amplitude of the strain pulse, and so the choice of the value of *A* becomes significant. For this reason, we have chosen *A* so that the simulation is in good agreement with the data for the highest pulse energy. The same value of *A* was then used in the simulations for lower pulse energy. In earlier picosecond ultrasonic experiments with Al films,[20] we have found that a good fit to echo pulse shapes can be obtained with $\phi=3.95$ radians, and this same value was used here. For each sample, the value of α was chosen to give a best fit. Changes in α primarily affect the rate at which the oscillations in the tail of the pulse shape decay, i.e., they do not have a large effect on

the shape of the soliton. If we set $A=\pi r^2$, we find that the values of A for the four samples correspond to radii r that lie in the range between 10 and 13.7 μm. Once the value of A is determined, the amplitude of the initial strain pulse is set. For example, with A having value corresponding to $r=13.6$ μm, a pump pulse energy of 0.37 nJ gives a strain amplitude in silicon of 3.5×10^{-5}.

It can be seen from Figs. 2–5 that the agreement between the simulations and the data is good, although not all features are accurately reproduced. Part of the discrepancy may arise from the use of a simulation in one dimension to approximate a three-dimensional problem. A full three-dimensional simulation would require a significant computational effort.[21] As the strain pulse propagates into the sample, it will spread laterally, and of course this diffraction is not considered in a one-dimensional simulation. For a Fourier component of wavelength λ and a source of radius r, diffraction becomes important after a propagation distance of $D\sim r^2/\lambda$. In the experiments reported here, the radius of the source is $\sim$15 μm, and the wavelengths of the components making up the strain pulse are typically in the range 0.05 to 0.1 μm. Thus, D is between 2 and 4 mm. It can be seen from Table II that the effect of diffraction should be small for Si and MgO (acoustic path less than 1 mm), but significant for quartz and sapphire (acoustic paths of 4 and 2 mm, respectively). A second effect that is neglected in the one dimensional model arises from the variation of the soliton amplitude with lateral position within the area excited by the pump. The probe beam has a radius of around 7 μm, and is centered on the pump beam. If we suppose that the pump beam has a Gaussian profile with a radius to half intensity of 15 μm, the sound amplitude at a distance of 7 μm from the center will be 14 % less than at the center. This variation in amplitude means that the soliton amplitude will be slightly larger at the center and so the soliton generated there will travel faster than a soliton generated away from the center. This spread in soliton velocities presumably has the consequence that the experimentally measured soliton component should be somewhat broader than is calculated in the one-dimensional simulation. We have not tried to apply a correction for this effect.

ACKNOWLEDGMENTS

This work was supported in part by the U.S. Department of Energy through Grant No. DE-FG03-ER45267. We thank Jamison Moeser for help with the theory of solitons.

[1] J. Robison and J. S. Russel, *Report of the Committee on Waves, Rep. 7th Meeting of British Association for the Advancement of Science*, Liverpool, 1838 (John Murray, London, 1838), p. 417.
[2] D. J. Korteweg and G. de Vries, Philos. Mag. **39**, 422 (1895).
[3] N. J. Zabusky and M. D. Kruskal, Phys. Rev. Lett. **15**, 240 (1965).
[4] M. J. Ablowitz, D. J. Kaup, A. C. Newell, and H. Segur, Phys. Rev. Lett. **31**, 125 (1973); Stud. Appl. Math. **53**, 249 (1974).
[5] D.C. Wallace, in *Solid State Physics*, edited by H. Ehrenreich, F. Seitz, and D. Turnbull (Academic, New York, 1970), Vol. **25**, p. 301.
[6] J. H. Cantrell and K. Salama, Int. Mater. Rev. **36**, 125 (1991).
[7] Note that we have used a symmetrized form for the Aabgdez coefficients.
[8] G. B. Whitham, *Linear and Nonlinear Waves* (Wiley, New York, 1974), Chap. 1.
[9] *Solitons in Action*, edited by K. Lonngren and A. Scott (Academic, New York, 1978).
[10] For a more complete review, see M. J. Ablowitz and H. Segur, *Solitons and the Inverse Scattering Transform* (SIAM, Philadelphia, 1981).
[11] As we will discuss in the next section, we cannot produce a pulse of this very simple shape with the generation method used in this paper.
[12] The amount of light transmitted through the Al film is small.
[13] Guray Tas and Humphrey J. Maris, Phys. Rev. B **49**, 15046 (1994).
[14] C. Thomsen, H. T. Grahn, H. J. Maris, and J. Tauc, Phys. Rev. B **34**, 4129 (1986).
[15] H. J. McSkimin, J. Appl. Phys. **24**, 988 (1953); H. J. McSkimin, P. Andreatch, Jr., and R. N. Thurston, *ibid.* **36**, 1624 (1965).
[16] *Landolt-Börnstein, New Series III/2* (Springer Verlag, Berlin, 1969).
[17] H. J. McSkimin and P. Andreatch, Jr., J. Appl. Phys. **35**, 3312 (1964); **37**, 267 (1966).
[18] We have measured the γ for Si, quartz, and sapphire and the results are reported in a separate paper [H.-Y. Hao and H. J. Maris, Phys. Rev. B **63**, 224301 (2001)]; for MgO we estimated an approximate value from Fig. 5.1(a) of H. Bilz and W. Kress, *Phonon Dispersion Relations in Insulators*, edited by M. Cardona and P. Fulde (Springer, New York, 1979), p. 50.
[19] In *Handbook of Optical Constants of Solids*, edited by A. D. Palik (Academic, Orlando 1985), which gives $n=2.8$ and $k=8.45$ for Al at the wavelength of 800 nm.
[20] H.-Y. Hao, H. J. Maris, and D. K. Sadana, Electrochem. Solid-State Lett. **1**, 54 (1998).
[21] Solitons in two dimensions have been considered by B. B. Kadomtsev and V. I. Petviashvili, Sov. Phys. Dokl. **15**, 539 (1979).